A New Criterion to Improve Operational Drizzle Detection with Ground-Based Remote Sensing

CLAUDIA ACQUISTAPACE AND ULRICH LÖHNERT

University of Cologne, Cologne, Germany

MAXIMILIAN MAAHN

University of Colorado Boulder, and NOAA/Earth System Research Laboratory, Boulder, Colorado

PAVLOS KOLLIAS

School of Marine and Atmospheric Sciences, Stony Brook University, State University of New York, Stony Brook, New York, and University of Cologne, Cologne, Germany

(Manuscript received 6 September 2018, in final form 16 January 2019)

ABSTRACT

Light shallow precipitation in the form of drizzle is one of the mechanisms for liquid water removal, affecting cloud lifetime and boundary layer dynamics and thermodynamics. The early formation of drizzle drops is of particular interest for quantifying aerosol–cloud–precipitation interactions. In models, drizzle initiation is represented by the autoconversion, that is, the conversion of liquid water from a cloud liquid water category (where particle sedimentation is ignored) into a precipitating liquid water category. Various autoconversion parameterizations have been proposed in recent years, but their evaluation is challenging due to the lack of proper observations of drizzle development in the cloud. This work presents a new algorithm for Classification of Drizzle Stages (CLADS). CLADS is based on the skewness of the Ka-band radar Doppler spectrum. Skewness is sensitive to the drizzle growth in the cloud: the observed Gaussian Doppler spectrum has skewness zero when only cloud droplets are present without any significant fall velocity. Defining downward velocities positive, skewness turns positive when embryonic drizzle forms and becomes negative when drizzle starts to dominate the spectrum. CLADS identifies spatially coherent structures of positive, zero, and negative skewness in space and time corresponding to *drizzle seeding*, *drizzle growth/nondrizzle*, and *drizzle mature*, respectively. We test CLADS on case studies from the Jülich Observatory for Cloud Evolution Core Facility (JOYCE-CF) and the Barbados Cloud Observatory (BCO) to quantitatively estimate the benefits of CLADS compared to the standard Cloudnet target categorization algorithm. We suggest that CLADS can provide additional observational constraints for understanding the processes related to drizzle formation better.

1. Introduction

Due to their radiative effects, boundary layer liquid clouds are responsible for the largest uncertainties in climate predictions (Bony et al. 2006); they scatter the incoming solar shortwave radiation that would be absorbed lower in the atmosphere or at the surface if the cloud was not present, leading to a cooling effect compared to cloud-free situations (Randall et al. 1984). The radiative properties of liquid clouds depend on how the cloud liquid water content is distributed horizontally and vertically in space. However, drizzle formation can modify cloud water content distributions by removing water content from the cloud; it can also alter in this way the cloud lifetime and the cloud cover, with direct effects on the radiation and also on the thermodynamical structure of the planetary boundary layer (PBL).

Drizzle plays a central role in the description of PBL liquid clouds in general circulation models (GCMs). However, drizzle is generally overestimated in GCMs (Ahlgrimm and Forbes 2014), having thus an impact on the amount of precipitation produced. In GCMs, the

Denotes content that is immediately available upon publication as open access.

Corresponding author: Claudia Acquistapace, cacquist@meteo.uni-koeln.de

DOI: 10.1175/JTECH-D-18-0158.1

autoconversion parameterization describes typically the growth of a droplet from cloud size to a precipitating size by means of collisions/coalescence with other cloud droplets. Normally, the autoconversion parameterization provides the rate at which drizzle drops are formed per unit time; different autoconversion parameterizations have been developed (Kessler 1969; Tripoli and Cotton 1980; Khairoutdinov and Kogan 2000; Liu and Daum 2004; Seifert and Beheng 2006; Franklin 2008), but several studies show that the autoconversion rates provided by the various schemes differ up to three orders of magnitude (Wood 2005; Hsieh et al. 2009). Some of the differences exist because autoconversion schemes are developed for different model resolutions and hence exhibit a scale dependency: at low resolutions, the average liquid water content (LWC) is lower and the autoconversion process needs to be triggered at a lower value compared to a scheme adapted to a higher-resolution model that can model higher LWC values. Recent observations show higher amounts of drizzle in clouds compared to models, that is, 83% of the observed marine stratocumuli from the ARM ground-based observatory on Graciosa Island in the Azores produce drizzle (Yang et al. 2018). Therefore, observations of the cloud to drizzle transition are needed to provide initial data for understanding aerosol–cloud–precipitation interactions and for evaluating autoconversion schemes after adjusting the observations to the scales at which a particular scheme is applicable.

To pursue this goal, various platforms are used for observing drizzle formation. Aircraft in situ measurements (e.g., Vogelmann et al. 2012; Siebert et al. 2013) can provide insights into drizzle formation, but such observations cannot provide a statistical characterization of the drizzle formation process due to the limited size of the in situ datasets. Satellite measurements (e.g., Stephens and Haynes 2007; L'Ecuyer et al. 2009; Suzuki et al. 2010) offer a global coverage, but are less sensitive to signals coming from atmospheric layers closer to the ground and have a coarse resolution (Rapp et al. 2013). Ground-based sensors can observe atmospheric profiles highly resolved in time and space which makes them particularly suitable for model evaluations.

The Cloudnet project was started in 2001 (http://devcloudnet.fmi.fi/) with the goal of using observations for the evaluation of cloud and aerosol profiles in numerical weather prediction (NWP) models. The Cloudnet algorithm package (Illingworth et al. 2007) constitutes now a branch of the European Research Infrastructure for the observation of Aerosol, Clouds, and Trace gases (ACTRIS) network (www.actris.eu), providing high-quality data and research infrastructures for observing aerosols, clouds, and trace gases; the Cloudnet package provides retrievals of liquid and ice water content (Hogan et al. 2006) and drizzle microphysical properties (O'Connor et al. 2005), at a very high temporal resolution (30 s) in quasi–real time and in standardized format. An additional product is the Cloudnet target classification, which is part of the Cloudnet algorithm suite and operationally determines drizzle presence within the cloud and below cloud base. The Cloudnet tool is used for many different applications: Ahlgrimm and Forbes (2014) exploit Cloudnet for validating GCMs, but the discrimination between drizzle and nondrizzle is also needed for applying microphysical retrievals. Due to its simple approach based on reflectivity thresholds, the Cloudnet target classification often provides physically inconsistent profiles that may not match with collocated liquid water path (LWP) observations from a microwave radiometer (MWR) (Acquistapace 2017). An improvement of the Cloudnet algorithm for drizzle detection from the ground should prove useful in model evaluation and to reduce uncertainties in the microphysical retrievals.

In recent years, various ground-based techniques have been developed to improve drizzle detection from the ground. Some exploit synergies of radar and lidar observations (O'Connor et al. 2005; Westbrook et al. 2010); other approaches combine microwave radiometers and cloud radars. Most are based on a reflectivity threshold to discriminate drizzle presence (Frisch et al. 1995b; Mace and Sassen 2000); Liu et al. (2008) link the threshold in reflectivity to the cloud droplet number concentration. However, the usage of reflectivity thresholds for observational discrimination of drizzle is always prone to calibration issues and biases occurring in the radar reflectivity measurements. Moreover, reflectivity may not be sufficient alone to properly detect drizzle presence. In recent years Kollias et al. (2011a,b) and Luke and Kollias (2013) suggested using higher moments of the radar Doppler spectrum to detect drizzle in liquid clouds. They introduced the skewness of the Doppler spectrum obtained from Ka-band radars. The skewness is sensitive to early drizzle production and drizzle growth throughout the cloud. Typically, cloud droplets without any significant fall velocity but under the influence of turbulence generate a Gaussian Doppler spectrum with skewness zero. The onset of drizzle leads to a deviation from the ideal Gaussian form. Using a convention of sign where downward velocities are defined positive, the embryonic formation of the first drizzle droplets causes the skewness to turn positive. The drizzle drops contribute to the formation of a long

tail in the radar Doppler spectrum at positive Doppler velocities, which causes an asymmetry of the spectrum shape to the right. While drizzle drops grow in size, the skewness turns from positive to negative values when drizzle starts dominating the spectrum. Despite its potential, the skewness variable is not yet used operationally to detect drizzle development in the clouds. Partly, this is related to the inherent noise that affects this variable and the variable's sensitivity to turbulence. Acquistapace et al. (2017) investigated optimal Ka-band radar settings to minimize the noise in the skewness to observe microphysical information best. They also quantified the impact of turbulence on the skewness signal for the purpose of drizzle detection.

This work presents a new criterion for drizzle detection which exploits the skewness for operational applications. The new criterion does not depend on a radar reflectivity threshold making it robust to errors in radar calibration; it identifies coherent structures of positive, zero, and negative skewness values in space and time, which correspond to different stages of drizzle droplet development. The new criterion is designed to extend and improve the Cloudnet target classification and similar cloud phase retrievals (e.g., Shupe et al. 2004) in detecting early drizzle developments by means of the skewness. We evaluate the new criterion using case studies with continental and maritime clouds as well as an ensemble of liquid cloud observations collected at the Jülich Observatory for Cloud Evolution Core Facility (JOYCE-CF) site, in Germany (Löhnert et al. 2015), and at the Barbados Cloud Observatory (BCO), in Barbados (Stevens et al. 2016).

The paper is organized as follows. In section 2, we describe the instruments and we also show the potential of skewness for an earlier detection of drizzle compared to the other radar Doppler moments based on a large ensemble of ground-based observations from JOYCE-CF. In section 3, we describe the new criterion in detail, while in section 4 we show the performance of the new criterion for continental and maritime clouds using case studies, as well as on a large ensemble of data. To quantify the improvements of the new criterion, we provide a comparison with the common Cloudnet target classification, and an evaluation based on independent microwave radiometer LWP observations. Finally, conclusions are drawn and future work is described in section 5.

2. Instruments and data

We use observations from a Ka-band microwave radar (MIRA) Doppler cloud radar operating in zenith-pointing mode deployed at the JOYCE-CF (Löhnert et al. 2015) (called JOYRAD-35) and at BCO (Stevens et al. 2016). MIRA collects Doppler spectra between cloud base and cloud top as a function of Doppler velocity v with 256 FFT points and an integration time of 1 and 10 s at JOYCE-CF and BCO, respectively. We process the Doppler spectra following the methodology described in Acquistapace et al. (2017) to estimate the radar Doppler spectra noise floor and to identify the signal of hydrometeors. Then the Doppler moments equivalent radar reflectivity factor (z_e and Z_e when expressed in dBZ), mean Doppler velocity V_d, Doppler spectrum width S_w, and skewness S_k are calculated from the Doppler spectra with noise removed $S(v)$ ($\mathrm{mm^6\,s\,m^{-4}}$) as follows:

$$z_e = \int_{-v_N}^{v_N} S(v)\,dv, \tag{1}$$

$$V_d = \frac{1}{z_e}\int_{-v_N}^{v_N} S(v)v\,dv, \tag{2}$$

$$S_w = \sqrt{\frac{1}{z_e}\int_{-v_N}^{v_N} S(v)(v - V_d)^2\,dv}, \tag{3}$$

and

$$S_k = \frac{1}{z_e (S_w)^3}\int_{-v_N}^{v_N} S(v)(v - V_d)^3\,dv, \tag{4}$$

where v_N is the Nyquist velocity (e.g., Doviak and Zrnić 1993).

To derive the LWP in the observed clouds, we use measurements obtained from a Humidity and Temperature Profiler (HATPRO) (Rose et al. 2005) microwave radiometer with a time resolution of 1 s. The same instrument is deployed at JOYCE-CF and BCO and the same retrieval algorithm type for LWP is applied (Löhnert and Crewell 2003). Typical uncertainties in LWP measurements are $20\,\mathrm{g\,m^{-2}}$ for the 7-channel retrieval adopted in this work. We use cloud base detected by a Vaisala CT25K ceilometer (Münkel et al. 2007) operating with a time resolution of 15 s at both sites. Cloud top is detected by the cloud radar. The Cloudnet package is operational at JOYCE-CF and it has been applied to BCO as well. The Cloudnet target categorization (Hogan and O'Connor 2004; Illingworth et al. 2007) detects cloud phase, aerosol presence, and precipitation with a time resolution of 30 s based on the synergy of cloud radar, microwave radiometer, and ceilometer observations. Here, we use the Cloudnet target classification to identify liquid clouds and to assess the new algorithm. All data are

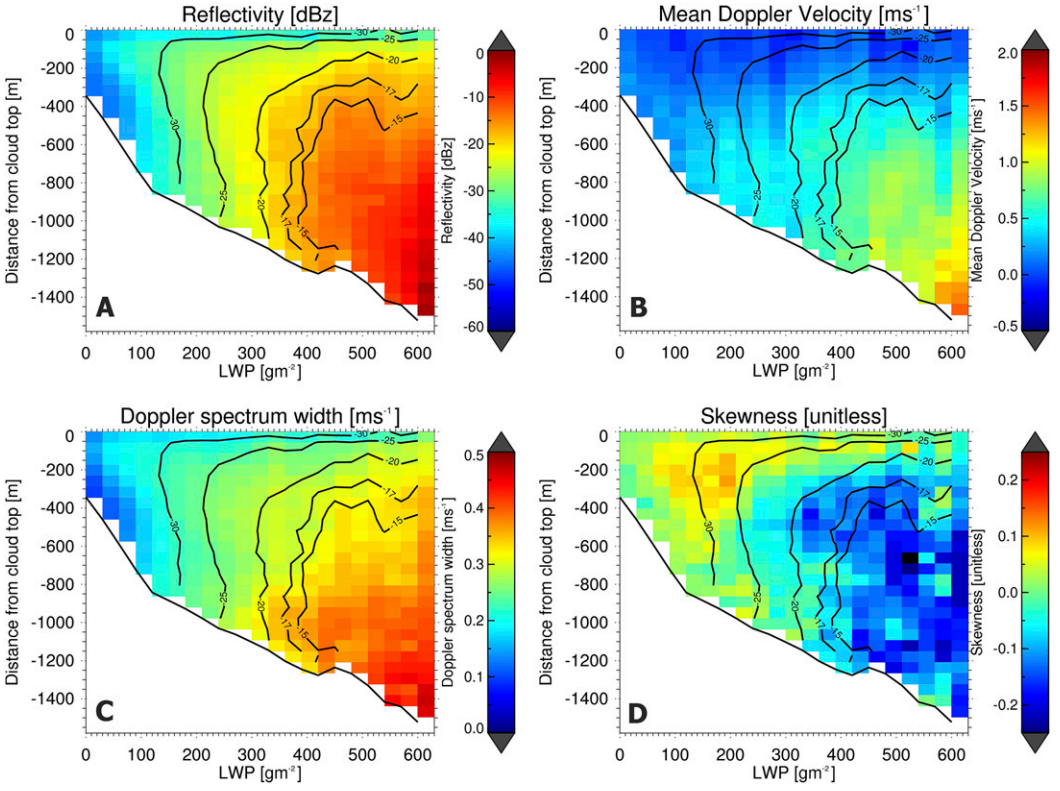

FIG. 1. Characterization of drizzle development for a dataset of 500 h of continental liquid clouds collected at JOYCE-CF: (a) Reflectivity mean values binned in terms of LWP and distance from cloud top. (b) As in (a), but for mean Doppler velocity. (c) As in (a), but for Doppler spectrum width. (d) As in (a), but for skewness. Black contour lines denote constant contours of reflectivity values.

interpolated to 1 and 10 s for JOYCE-CF and BCO, respectively.

We use a dataset of 500 h of continental liquid drizzling and nondrizzling clouds at JOYCE-CF collected between 2013 and 2015. Figure 1 shows the characterization of the drizzle development in the liquid cloud dataset in terms of LWP, reflectivity, mean Doppler velocity, Doppler spectrum width, skewness, and distance from cloud top. We provide an interpretation of the radar observables and implications for the cloud microphysics as follows. For LWP values smaller than 100 g m^{-2}, the mean observed values of radar Doppler moments indicate a typical adiabatic cloud profile; small values of reflectivity below −30 dBZ increase from cloud base (identified by the black line) to cloud top due to the diffusional growth that droplets undergo while rising. The ascending motions are indicated by the observed negative values of mean Doppler velocity (positive velocities in the convention used in this work are directed downward) and Doppler spectrum width mean values increase from cloud base to cloud top, due to the broadening of the Doppler spectrum width induced by turbulence. Skewness values are approximately zero throughout the profile because no microphysical signatures of drizzle formation are present; LWP values observed in this range are typical of nondrizzle regimes (Acquistapace 2017).

For LWP between 100 and 250 g m^{-2}, the microphysical signature of drizzle is visible in the observations: values of reflectivity range between −30 and −25 dBZ and are homogeneous with height. Since Z_e is proportional to the sixth power of the droplet diameter, larger Z_e may be due to the presence of a few bigger droplets. Such droplets are also responsible of the larger Doppler spectrum width through the whole cloud vertical profile. Mean Doppler velocity values close to cloud top are still negative indicating updrafts. In the lower part of the cloud, hydrometeors grow due to the collision–coalescence process, start to fall, and V_d shows positive values (downward). Skewness shows a clear positive feature within the first 200 m below cloud top. This is the microphysical signature of drizzle seeding, (also known as embryonic drizzle formation) (Luke and Kollias 2013). No corresponding variations in the other Doppler

moments are visible which shows that skewness has the potential to detect drizzle formation earlier compared to other variables. Going toward cloud base, the mean S_k values decrease again toward zero. On average, no negative skewness values are observed in this range of LWP values. The absence of negative skewness values in the column suggests that drizzle droplets formed aloft have not fully grown to become precipitating drops. This lack of precipitation formation may be due to various reasons: first, the radar volume can be filled with cloud droplets and some drizzle particles not large enough to have an appreciable fall velocity; second, drizzle formed in updrafts might evaporate when reaching cloud top due to the entrainment of dry air; and third, the cloud has a too-small vertical extension.

For LWP larger than 250 g m^{-2}, all radar moments indicate the development of precipitation. The Z_e increases from cloud top toward cloud base and mean Doppler velocity increases from zero to values between 0.7 and 2.0 m s^{-1} (downward) from cloud top to cloud base. Doppler spectrum width grows from cloud top to cloud base to values up to 0.3–0.4 m s^{-1}, which might be due to larger drops or turbulence induced by the falling hydrometeors, or by a broadening of the droplet size spectrum. Finally, mean skewness shows a full transition from positive values at cloud top to negative values already 200 m below cloud top. The narrow transition from positive to negative values occurring already 200 m below cloud top shows that in the presence of sufficient liquid water with a larger vertical extension, embryonic drizzle grows fast to form precipitating droplets. In this situation, the precipitation is dominating the radar signal and producing negative skewness values and conceals the signature of drizzle formation. Therefore, when skewness turns negative, drizzle can continue to form in the presence of precipitation and it might not be detected from the radar. The contour lines of radar reflectivity clearly highlight how late in the process of drizzle formation typical Z_e thresholds of −20 to −15 dBZ are able to detect drizzle. The detection threshold of −20 dBZ proposed by Kogan et al. (2005) captures almost the entire region of negative skewness values, while other thresholds normally used (−17 dBZ in Frisch et al. 1995a) miss some negative skewness areas. It is interesting to note that positive skewness signatures occur already for radar reflectivities of −30 dBZ. An example of the evolution of the radar Doppler spectrum for the cloud to drizzle transition is shown in Fig. 2. While the radar reflectivity fluctuates between −25 and −22 dBZ between cloud top and cloud base, the skewness shows a transition from positive to negative

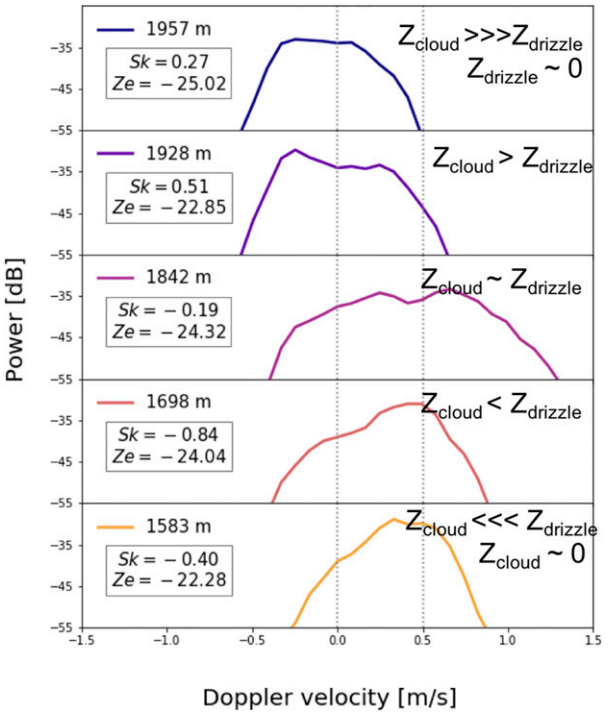

FIG. 2. Example of the evolution of the radar Doppler spectrum through the cloud observed at 0748 UTC 30 Jun 2013 at the JOYCE-CF. Close to cloud top (1957 m), the Doppler spectrum is approximately symmetrical and skewness is close to zero (0.27). Within 100 m from cloud top, the skewness turns positive while the drizzle contribution increases and at 1842 m the skewness becomes negative (−0.19). There, the shape is broadened by the two peaks corresponding to cloud droplets and drizzle. Further down, at 1698 m and lower at 1583 m, the radar Doppler spectrum is dominated by drizzle and the skewness shows high negative values (−0.84 and −0.40, respectively).

values moving from cloud top to cloud base, with four different stages:

- a near-zero skewness regime with very low total reflectivity values, mainly due to the cloud component of reflectivity (Z_{cloud}) with nondetectable reflectivity due to drizzle (Z_{drizzle}) corresponding to the *nondrizzle* class;
- a positive skewness regime with a slightly higher total reflectivity and $Z_{\text{drizzle}} < Z_{\text{cloud}}$, which we refer to as *drizzle seeding*;
- a near-zero skewness class with higher radar reflectivity and $Z_{\text{drizzle}} \approx Z_{\text{cloud}}$, corresponding to *drizzle growth*; and
- a negative skewness regime with highest radar reflectivities, corresponding to $Z_{\text{drizzle}} > Z_{\text{cloud}}$, referred to as *drizzle mature.*

The statistical analysis, as well as the example shown in Fig. 2, thus reveals that drizzle presence can be

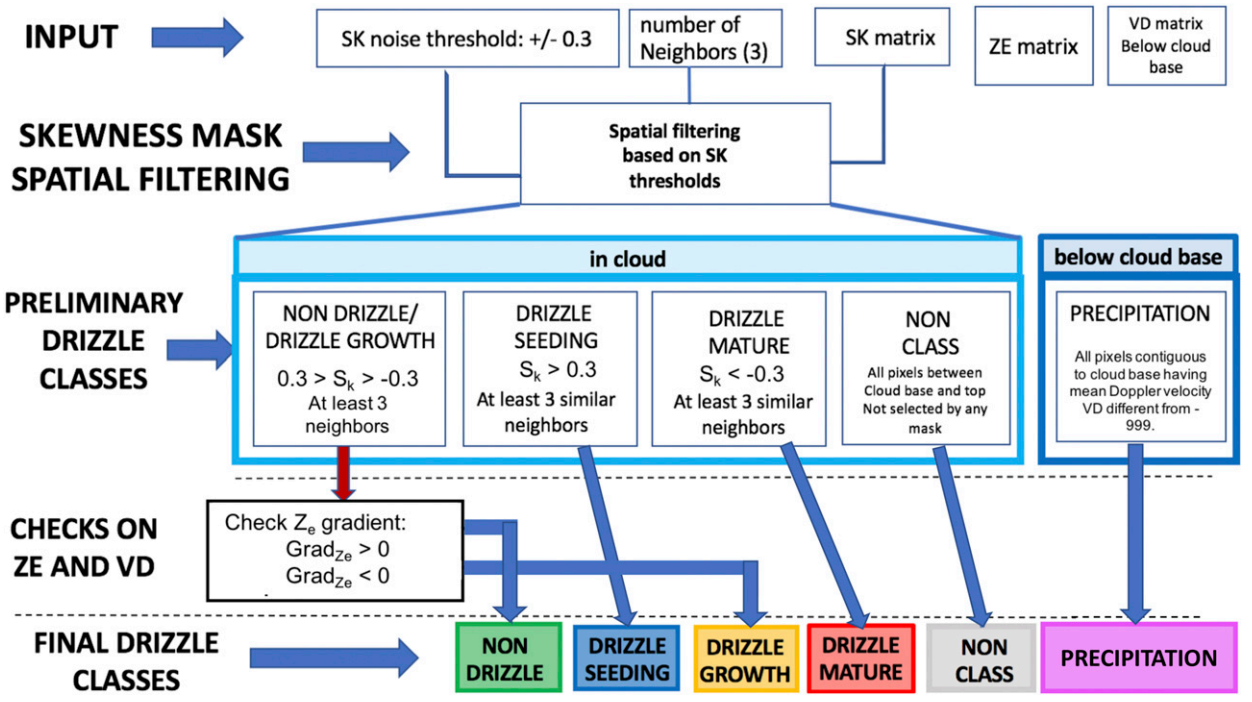

FIG. 3. Flowchart of the algorithm for the Classification of Drizzle Status (CLADS).

detected by skewness at an earlier stage compared to the other radar Doppler moments.

3. The new algorithm for CLADS

The skewness is the third moment of the radar Doppler spectrum; thus, it is a noisy moment. Such noise is due to radar data processing and/or dynamical motions and can induce erroneous detection of microphysical signatures. The algorithm for Classification of Drizzle Stages (CLADS) uses the concept of a spatial filter on skewness values to identify different stages of drizzle development in the cloud reliably. When provided with a given number of neighboring

TABLE 1. Variables and parameters used in the CLADS algorithm.

Variables to be provided to CLADS	Source for this work	Motivation for the variable
Skewness	MIRA Doppler spectra	Input for CLADS mask to be read and filtered
Reflectivity	MIRA Doppler spectra	Calculation of gradient of reflectivity
Mean Doppler velocity	MIRA Doppler spectra	Detection of precipitation below cloud base
Cloud base	Cloudnet algorithm	Identification of the area where CLADS is applied
Cloud top	Cloudnet algorithm	Upper limit of the area where CLADS is applied
Parameters to be provided to CLADS	**Values of parameters used in this work**	**Meaning of the parameter**
$n_{\text{neighbors}}$	3	Number of pixels with same conditions on skewness needed to assign a drizzle class
$S_{k_{\text{thr}}}$	0.3	Threshold value for skewness used to separate nondrizzle/drizzle growth classes from drizzle onset/drizzle mature
Portion of Z_e profile to exclude for gradient calculation at cloud top and cloud bottom	20%	Portion of reflectivity profile used to estimate the reflectivity gradient.

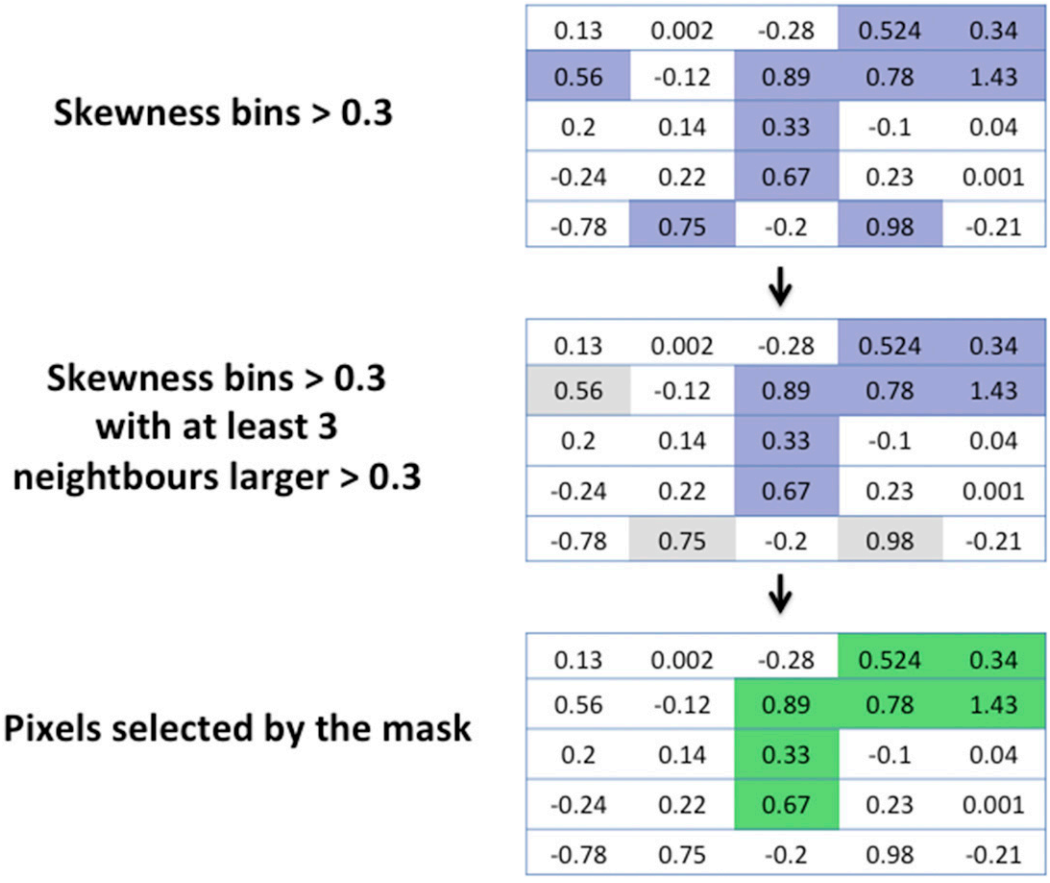

FIG. 4. Example showing the principle of the skewness mask for the drizzle onset category: purple boxes indicate pixels that are fulfilling the condition $S_k > 0.3$, gray boxes are pixels that are discarded by the coherent structure filler. Green boxes represent the final selection of pixels from the mask.

pixels $n_{\text{neighbors}}$, the filter identifies coherent structures in space and time of positive, zero, and negative skewness values. Additional conditions are then applied to determine the different drizzle development stages. The inputs for CLADS are skewness, mean Doppler velocity and reflectivity gradient fields, cloud base, and cloud top. In addition, the user needs to define a skewness threshold to discriminate noise and the number of neighbors $n_{\text{neighbors}}$ to apply in the skewness mask. See Fig. 3 for an overview of the algorithm and Table 1 for the list of parameters to be provided by the user. Acquistapace et al. (2017) establish a threshold in skewness to discriminate microphysical signatures of drizzle development from turbulence-dominated skewness values. The threshold depends on the integration time and spectral resolution of the radar. For the radar settings used in this work the threshold is 0.3. The core of CLADS is the concept of the skewness mask, which is applied to the skewness time–height field between cloud base and cloud top for identifying coherent structures. Pixels are selected that satisfy a specified condition (i.e., $S_k > 0.3$ for drizzle seeding) and have at least $n_{\text{neighbors}}$ of 9 adjacent pixels also fulfilling the same condition. In this way, the mask detects coherent areas of similar skewness in time and height. The mask selects areas based on the following idea: when drizzle develops at one point in time–height, skewness signatures of drizzle presence are highly probable also in adjacent pixels. A sensitivity test was conducted to determine the number of neighbors. We used 2, 3, and 4 neighbors to verify how sensitive the algorithm is to such a parameter. We hardly saw any difference between 2 and 3 pixels, while we lost significant structures when using 4 pixels. Therefore, we chose 3 as the most consistent parameter. Figure 4 shows an example of the pixels selected by the skewness mask for $S_k > 0.3$ and $n_{\text{neighbors}} = 3$. Figure 4 clearly shows that the masking principle is effective in excluding isolated pixels with very high skewness values, which are often caused by noise.

We apply the skewness mask between cloud base and cloud top with the condition of skewness values larger

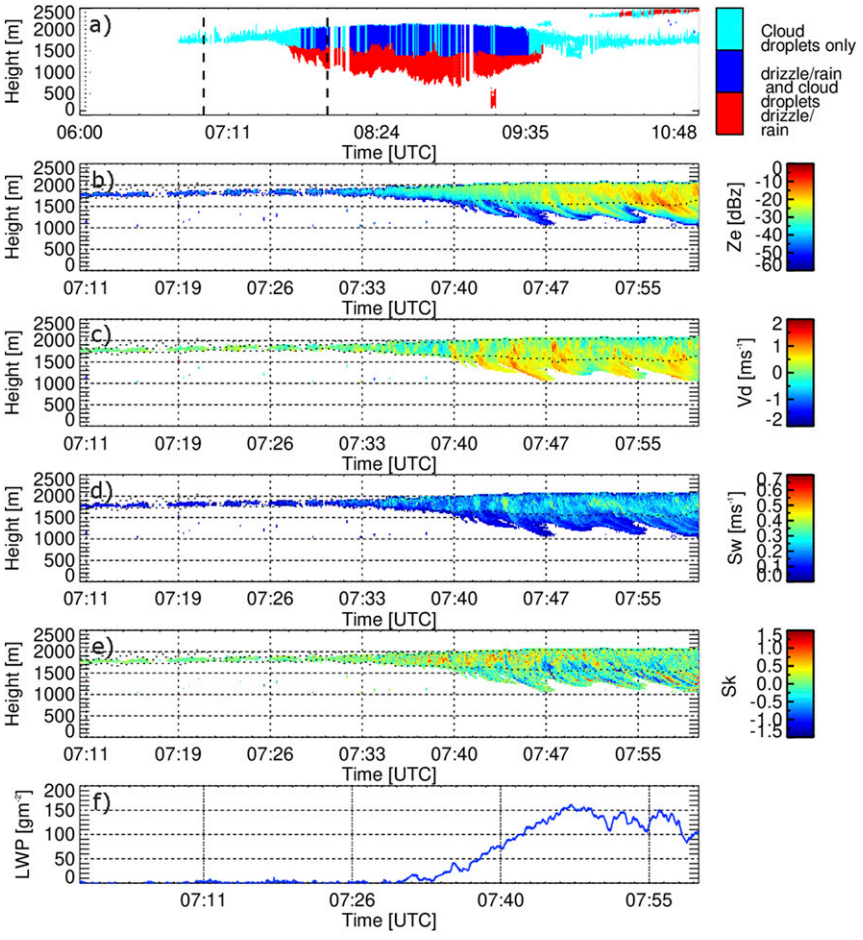

FIG. 5. Liquid cloud forming at the top of the boundary layer and developing some virga over JOYCE-CF on 30 Jun 2013. (a) Cloudnet target classification from 0600 to 1100 UTC showing the development of the cloudy layers and the formation of precipitation. The area between the two vertical dashed lines represents the hour selected as case study. (b) Reflectivity Z_e, (c) mean Doppler velocity V_d, (d) Doppler spectrum width S_w, (e) skewness S_k as a function of time and height for the selected hour, between 0700 and 0800 UTC, and (f) LWP time series between 0700 and 0800 UTC.

than 0.3 to detect early formation of small drizzle droplets (drizzle seeding), and with the condition of S_k values smaller than -0.3 to detect drizzle dominating the signal (drizzle mature). We also apply the skewness mask with the condition that values of skewness range between -0.3 and 0.3 to identify the nondrizzle/drizzle growth classes. This mask selects all the pixels whose S_k values are generated by the microphysical signature of cloud droplets only or by the equal coexistence of cloud droplets and drizzle in terms of Z_e, or by domination of turbulence.

After a preliminary classification of the drizzle classes based on skewness, we apply an additional test for distinguishing between nondrizzle/drizzle growth based on the vertical gradient of Z_e. Ground-based radar observations are prone to the limitation of being able to detect only vertical transport and only under certain conditions (i.e., no shear). Assuming absence of wind shear, for every column of time presenting a cloud, we exclude cloud-edge areas from the calculation of the gradient to avoid influences of entrainment and partial beam filling. For every pixel in these classes, we omit the upper and lower 20% of the profile and we calculate the mean Z_e gradient of the remaining reflectivity bins in the cloudy column. We remove profiles which result in less than 3 radar bins selected. In the absence of drizzle, the reflectivity of an adiabatic air parcel will increase with altitude because of the condensational growth of the cloud particles. We associate this positive gradient with nondrizzle conditions. When drizzle develops at some height in the cloud, the Z_e gradient is close to zero. Further drizzle growth

reverses the sign of the gradient. Consequently, pixels belonging to cloud columns with a negative gradient are assigned to the drizzle growth class. Drizzle growth is an intermediate stage in the drizzle formation where drizzle, even if present, is not yet dominating the Doppler spectrum and the skewness signature ($Z_{\text{cloud}} \approx Z_{\text{drizzle}}$).

The last two remaining classes of nonclassified and precipitation pixels are defined as follows: all pixels between cloud base and cloud top that are not selected by any skewness mask are classified as nonclassified. For nonclassified pixels, the observables used in this algorithm do not provide enough information to determine the stage of drizzle development unambiguously. Finally, all connected pixels below cloud base which show nonnull values of mean Doppler velocity are considered precipitation.

The final classes obtained by the CLADS algorithm are nondrizzle, drizzle seeding, drizzle growth, drizzle mature, nonclassified, and precip.

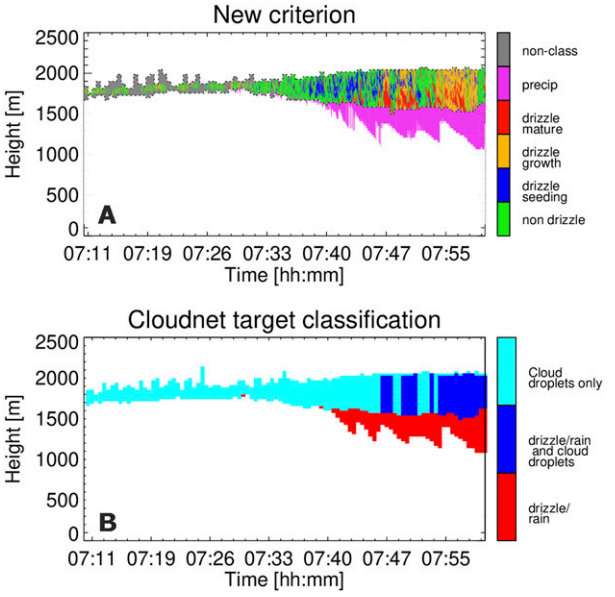

FIG. 6. (a) Classification of drizzle classes using the new criterion for the liquid cloud forming at the top of the boundary layer at JOYCE-CF between 0700 and 0800 UTC 30 Jun 2013. (b) Cloudnet target classification for the same hour.

4. Results

a. *Single case studies*

1) THIN LIQUID BOUNDARY LAYER CLOUD DEVELOPING LIGHT DRIZZLE

A single-layer liquid cloud develops at the top of the boundary layer in the early morning of 30 June 2013 (Fig. 5). The case is a typical development of light drizzle in a continental thin boundary layer cloud characterized by small turbulence. It forms at around 0700 local time (LT) and develops precipitation after 40 min. In 10 min starting from 0730 LT, cloud thickness increases from 100 to 300 m and LWP grows from 25 up to 100 g m^{-2}. Cloudnet captures the precipitation below cloud base and detects the presence of drizzle inside the cloud just a few minutes after precipitation below cloud base appears (lower panel of Fig. 6). Standard moments do not reveal evidence of drizzle formation: reflectivity values between 0730 and 0740 LT are homogeneously below −30 dBZ with just some small updrafts before 0740 LT, while some evident downdraft structures in V_d appear only after 0740 LT. The Doppler spectrum width field in the cloud presents spots of larger values that possibly indicate turbulence.

The new criterion describes the evolution of the drizzle droplets from cloud top to cloud base in a more detailed way than Cloudnet. Between 0730 and 0740 LT, most regions in the cloud are classified as drizzle seeding (Fig. 6). At 0742 LT, drizzle seeding occupies the upper part of the cloud, while in the lower part some drizzle mature pixels also appear. The remaining pixels in the cloud are classified as nondrizzle. The nondrizzle class is assigned because the size of the embryonic drizzle is too small, at that height in the cloud, to provide variations in the adiabatic Z_e profile and therefore the gradient parameter remains positive producing a local misclassification. At lower heights, few drizzle mature spots appear, indicating that the drizzle falling from the upper levels has grown to a size large enough to turn the skewness negative; hence, we might hypothesize that the drizzle is forming through the vertical column and falls out of the cloud as precipitation. In some areas, the precipitation found below nondrizzle cloudy areas is likely produced somewhere else in the cloud and advected into the observed column due to shear. In contrast to the new criterion, Cloudnet classifies the same observations as nondrizzle. After 0740 LT, large areas of pixels classified as drizzle mature appear in the lower half of the cloud. Drops grow larger in this region and the gradient of the Z_e profile changes sign. For this reason, the algorithm identifies most of the regions selected by the skewness mask (i.e., with skewness between −0.3 and 0.3) as drizzle growth and detects drizzle mature areas in the cloud, where precipitation forms. After 0740 LT Cloudnet detects drizzle between cloud base and cloud top, but cannot track the drizzle growth process and detect areas where larger droplets are located.

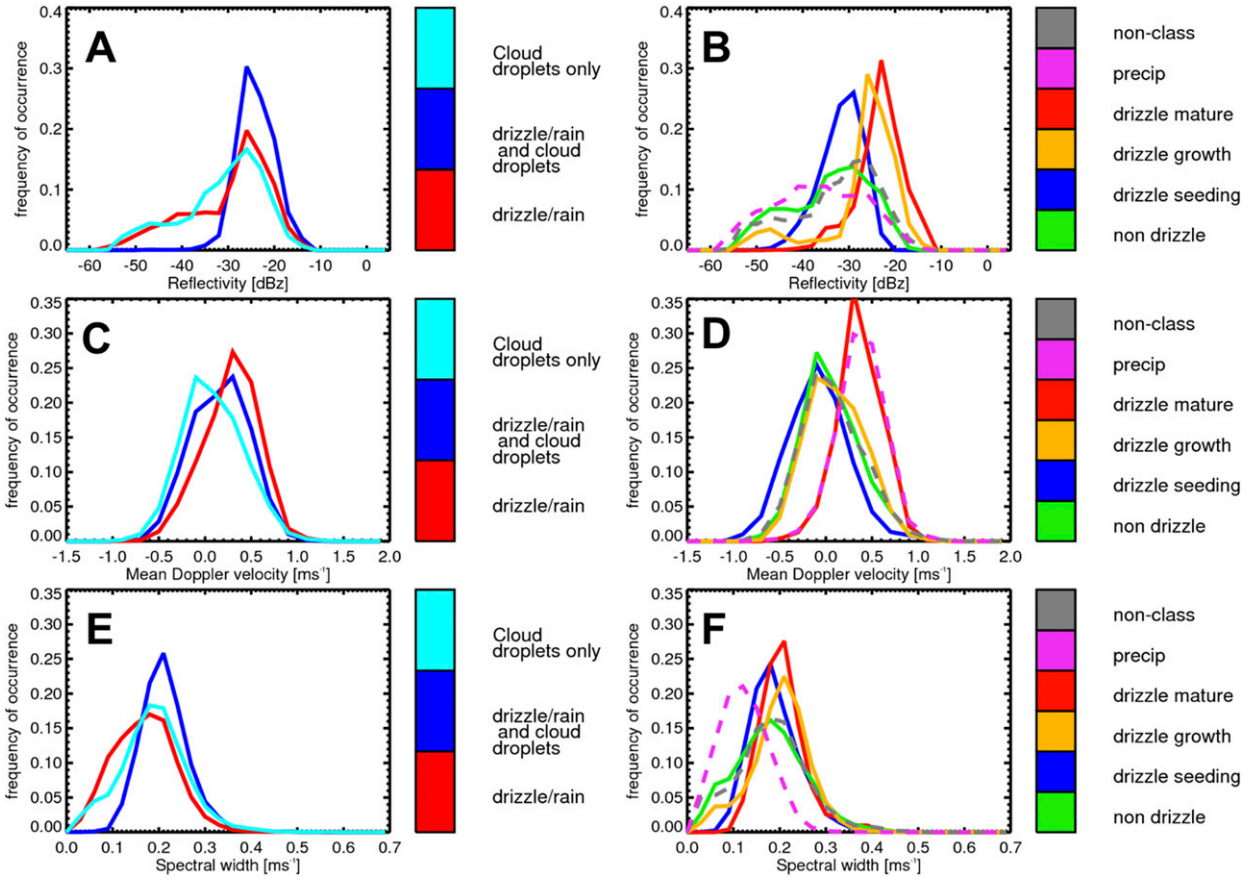

FIG. 7. Distributions of (a),(b) reflectivity, (c),(d) mean Doppler velocity, and (e),(f) Doppler spectrum width obtained for the Cloudnet target classification categories identifying (left) drizzle and (right) for the drizzle classes introduced by the new criterion for the liquid cloud forming at the top of the boundary layer at JOYCE-CF between 0700 and 0800 UTC 30 Jun 2013. Dashed lines represent discarded data.

Overall, the new criterion shows potential to track the evolution of the embryonic drizzle drops: this is also visible in the distributions of reflectivity obtained for the drizzle classes shown in Fig. 7b). For the new criterion, the nondrizzle distribution peaks at -30 dBZ while drizzle seeding shows Z_e values between -32 and -26 dBZ. The histograms of pixels belonging to the drizzle growth and the drizzle mature classes resemble the shape of the distribution obtained for drizzle seeding pixels, but they are shifted to larger values; 75% of drizzle growth pixels have Z_e between -26 and -20 dBZ and 75% of drizzle mature pixels have Z_e between -24 and -18 dBZ. The tiny peak observed in the drizzle growth distribution around -50 dBZ is likely due to biased skewness at low signal-to-noise ratios (SNRs). The three peaks for drizzle seeding, drizzle growth, and drizzle mature can be interpreted as the temporal evolution of an initial amount of embryonic drizzle droplets that increase their size in the cloud due to diffusional growth and collision–coalescence. Precipitation and discarded pixels are characterized by Z_e values spanning on a broad interval of Z_e values, from -55 to -11 dBZ. In contrast, Cloudnet categories of pixels are not clearly separated; all Cloudnet classes show a main peak of Z_e at -25 dBZ.

Also the mean Doppler velocity distributions (Figs. 7c,d) indicate that the new criterion identifies different stages of drizzle development. For the discussion, we can assume that the average mean Doppler velocity is a proxy for the hydrometeors fall velocity. The distributions of nondrizzle, drizzle seeding, nonclassified, and drizzle growth peak at $0\,\mathrm{m\,s^{-1}}$; that is, they do not fall on average. Such velocity values do not correspond to organized updraft or downdraft motions, but more to random displacements occurring in the cloud due to a slow adiabatic ascent, turbulence, and entrainment. In contrast, the drizzle mature and precipitation distributions peak at $0.35\,\mathrm{m\,s^{-1}}$ with a nonnegligible mean falling velocity. While the classes of the new criterion exhibit either a precipitating or a nonprecipitating

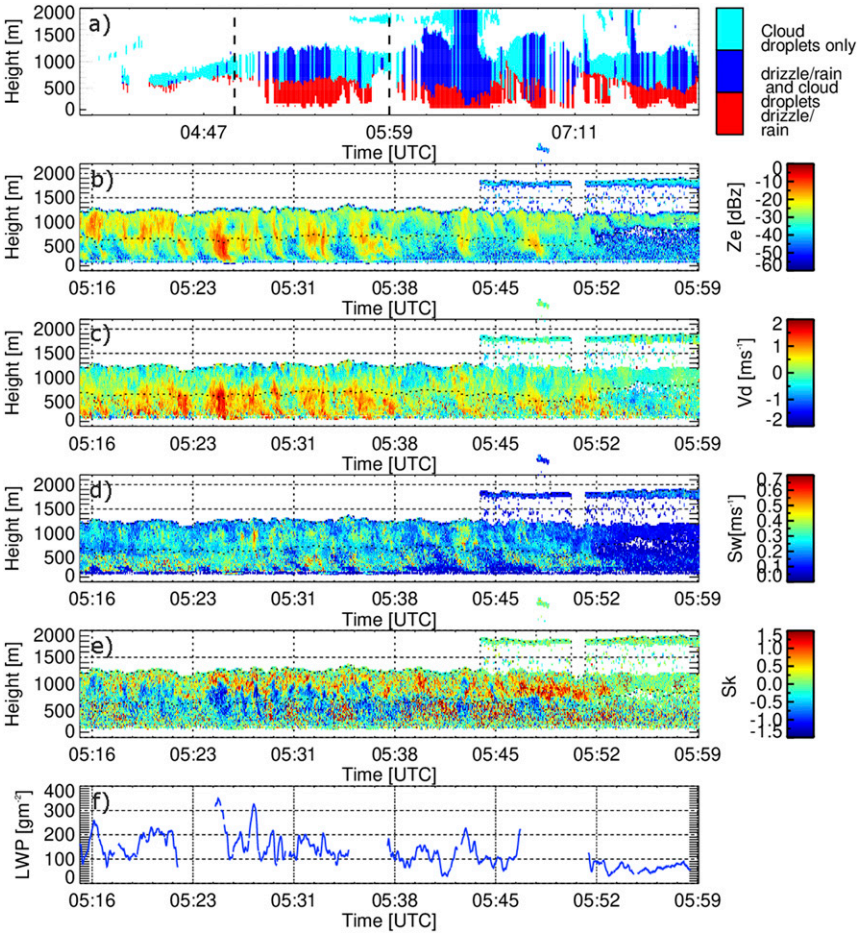

FIG. 8. As in Fig. 5, but for the thick drizzling stratus over JOYCE-CF on 21 Jul 2015.

peak, all mean Doppler velocity distributions for the Cloudnet categories show one single peak between 0 and 0.5 m s^{-1}. Doppler spectrum width is determined by the width of the combined drop drizzle size distribution, turbulence, and shear. In our observations however, it is not possible to disentangle the impact of turbulence from that of microphysics, therefore limiting our ability to interpret the observed signal. For the nondrizzle class of the new criterion, 25% of S_w values are less than 0.14 m s^{-1}. The Doppler spectrum width values around 0.2 m s^{-1} observed for the remaining distribution may indicate that turbulence is low in this case study. The very low values of Doppler spectrum width can be interpreted as the microphysical signature of a narrow size distribution of cloud droplets with small turbulence. The drizzle seeding, drizzle growth, and drizzle mature classes have very similar distributions peaking around 0.2 m s^{-1}. Assuming again that the turbulence in this case study is low, these distributions correspond to situations in which the presence of cloud droplets and drizzle broadens the radar Doppler spectrum; 75% of the precipitating drops have $S_w < 0.13$, indicating that precipitation is less affected by turbulence. For Cloudnet, the shape of the nondrizzle distribution resembles that for the nondrizzle class in the CLADS scheme. Cloudnet's drizzle/rain pixels show 25% of pixels with $S_w < 0.13$ and 50% of pixels with $S_w > 0.18$. In this case, the smaller S_w values are generated by monomodal precipitating drops, while the broader spectra may occur when rain develops causing larger S_w values; in Cloudnet, 80% of pixels of the drizzle/rain and cloud droplets distributions range between 0.18 and 0.29. In this case, larger values may be due to the coexistence of a cloud droplet and a drizzle peak in the radar Doppler spectrum.

2) THICK PRECIPITATING STRATUS CLOUD

In contrast to the previous case, this case study shows a thick continental stratocumulus cloud developing rain at JOYCE-CF on 21 July 2015. The cloud is first

observed in the morning hours (Fig. 8). After 0500 LT, cloud thickness increases and precipitation is initiated shortly. We analyze the period between 0500 and 0600 LT, where the LWP is generally larger than $100\,g\,m^{-2}$ with peaks up to $300\,g\,m^{-2}$. Vertical structures of large Z_e (up to -10 dBZ) extend from cloud top to cloud base. Mean Doppler velocity increases from $0\,m\,s^{-1}$ at cloud top to $2\,m\,s^{-1}$ at cloud base, indicating the presence of precipitation falling out of the cloud. Finally, Doppler spectrum width values during the selected period are on average smaller than $0.3\,m\,s^{-1}$, indicating low turbulence.

The larger cloud thickness compared to the case shown in Fig. 6 allows the development of strong precipitation. Unlike for the thin liquid cloud of case a.1, the drizzle seeding class is found constantly in the upper half of the cloud. This is probably where drizzle embryonic droplets form. They then slowly fall through the cloud and increase their size due to collision/coalescence. Since in this case, the LWP is larger than in the first example (Fig. 5 and Fig. 6), embryonic drizzle grows to larger size while falling. Between 0523 and 0531 LT, LWP often peaks above $200\,g\,m^{-2}$ corresponding to the larger drizzle mature areas and precipitation structures. Cloudnet (Fig. 9, bottom) detects also precipitation below cloud base but the classification in the cloud alternates between cloud droplets only, drizzle/rain, and cloud droplets without a relation to the LWP observations. Similar to the first case, the drizzle mature pixels of the new criterion have for the larger reflectivities (peak at -21 dBZ) as those having the larger reflectivities than the other classes (see Fig. 10b). Only for the drizzle growth and nondrizzle classes, there are 50% of pixels smaller than -30 dBZ; the drizzle seeding distribution peaks at -30 dBZ with only 25% of pixels smaller than -31 dBZ. The largest difference to the Z_e distributions of the first case is for the drizzle growth class that peaks below -20 dBZ with 50% of the pixels smaller than -30 dBZ. We provide here an interpretation which is coherent with the larger LWP observed in this case. This interpretation is also supported from the plots of skewness shown in Fig. 1, where we can observe that, when LWP is larger than $200\,g\,m^{-2}$, skewness shows a very fast transition from positive to negative values, which might be due to the large cloud thickness and LWP available. In this case, it might be that all the drizzle growth droplets with larger Z_e eventually form drizzle due to the larger amount of liquid water. This depletes the cloud part, induces a negative skewness, and contributes to the drizzle mature population. In the first case, the restricted amount of available liquid water limits the

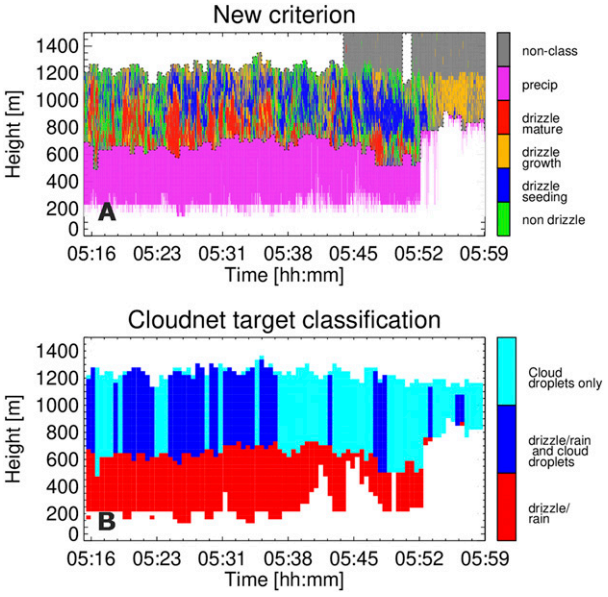

FIG. 9. As in Fig. 6, but for the thick drizzling stratus over JOYCE-CF between 0500 and 0600 UTC 21 Jul 2015.

growth of droplets. Hence, the cloud part is not depleted and the skewness values close to zero lead to a classification as drizzle growth. As in the first case, Z_e distributions for Cloudnet classes peak between -30 and -25 dBZ and are mostly superimposed. Overall, the new criterion shows a physically more consistent characterization of the different stages of drizzle development in terms of Z_e and V_d distributions.

3) SHALLOW CUMULUS LIQUID CLOUDS OVER BARBADOS

We investigate shallow cumulus cloud overpassing the Barbados site on 11 December 2013 (Fig. 11). The Cloudnet target classification identifies cloud droplets in the cloud and precipitation below cloud base (see Figs. 11 and 12). Observed Z_e values are generally larger compared to the previous continental stratus cases, due to the maritime nature of these cumuli. Larger Z_e and S_w values are observed close to cloud top. We can hypothesize that drizzle forms due to collision/coalescence occurring at cloud top, where turbulence is stronger due to cloud-top cooling. Larger drops have to fall through lower layers where V_d shows larger positive downward values. The larger values of S_w up to $0.7\,m\,s^{-1}$ suggest the presence of strong turbulence in this case. However, these large values may also be due to the 10-s integration time adopted at this site. The LWP observations are around $50\,g\,m^{-2}$ with peaks up to $100\,g\,m^{-2}$ shortly after 0700 LT that correspond to

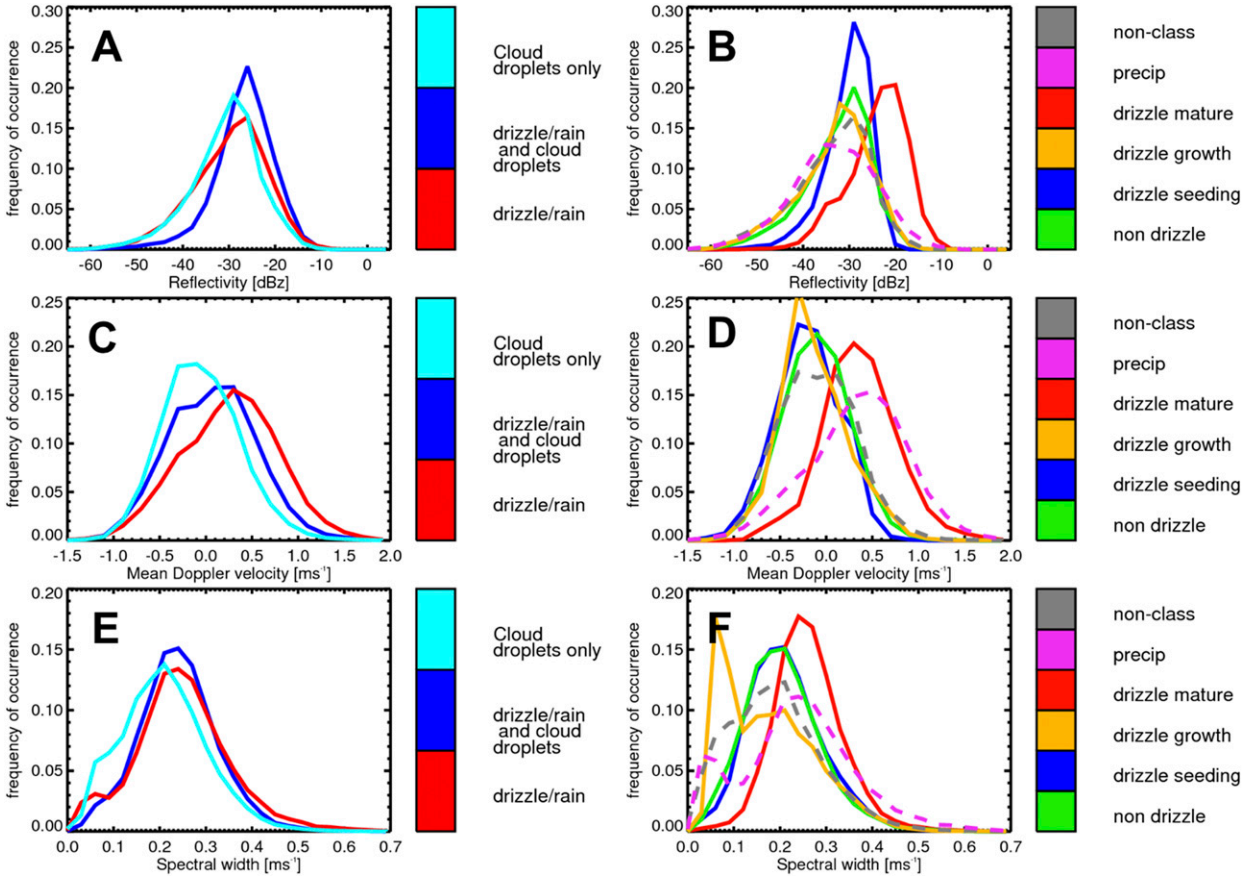

FIG. 10. As in Fig. 7, but for the thick drizzling stratus over JOYCE-CF on 21 Jul 2015.

the precipitating cloud occurring from 0700 to 0710 LT. Figure 12 shows an hour of comparison between the Cloudnet target classification and the new algorithm. The new criterion identifies pockets of drizzle seeding often close to cloud top while drizzle mature pixels are located very close to cloud base. In this case, the integration time used for the radar observations is 10 s. Together with the larger turbulence occurring at the Barbados site, this smooths the skewness signal (Acquistapace et al. 2017). This case study clearly shows how a coarse temporal resolution limits the performance of the new algorithm: only a few areas are identified as drizzle seeding and/or drizzle mature, while the majority of pixels are assigned to a class corresponding to skewness around zero.

Despite that, interesting features can be identified in the observations and areas classified as drizzle seeding and drizzle mature are still classified consistently. With high-resolution observations, however, more pixels would be likely classified as drizzle seeding and drizzle mature. From 0706 to 0711 LT, a drizzle seeding region located close to cloud top evolves toward cloud base in an area of zero skewness and is classified as drizzle mature around cloud base. The zero skewness region is identified by CLADS in a nonconsistent way as nondrizzle because the Z_e profile is still adiabatic. However, we expect to find drizzle and cloud droplets in these pixels following the hypothesis that drizzle forms at cloud top (as shown by the drizzle seeding areas) and then, it grows as it falls through the cloud. In this case, the number concentration might be too low to modify the Z_e profile, which remains adiabatic despite the presence of drizzle drops. This effect may be enhanced also by the fact that clouds droplets are larger in general for maritime clouds compared to continental ones. Below cloud base, precipitation with large mean Doppler velocity (see Fig. 11) is observed. Due to the lower number concentration that generally occurs in maritime clouds (Miles et al. 2000), drizzle drops can grow with less competition for the available liquid water compared to continental clouds. Moreover, the collision efficiency for larger drops is larger and the drizzle drops can reach larger sizes. Also, some rain below nondrizzle cloudy areas is found

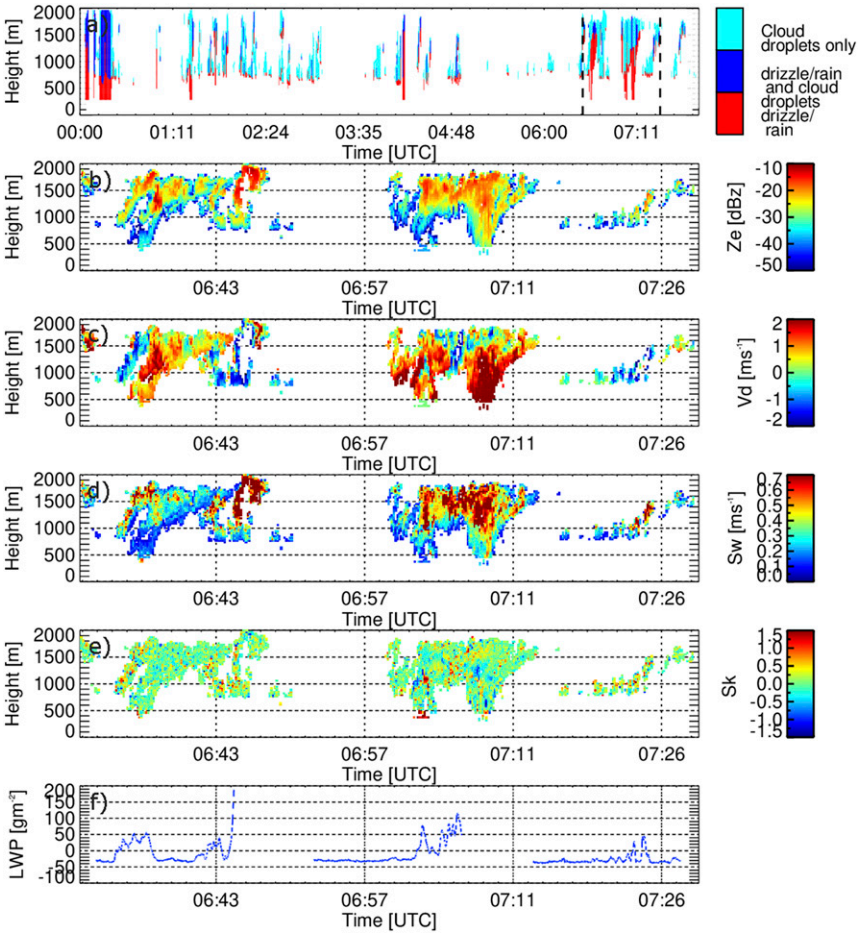

FIG. 11. As in Fig. 5, but for the shallow cumulus cloud over BCO on 11 Dec 2013.

around 0711 LT. This effect might be due to the combined effect of turbulence and long integration time that can dampen the skewness signatures. The Doppler spectrum width distributions clearly show how much CLADS is affected by turbulence and long integration times. The S_w maximum observed values are almost doubled compared to those observed in continental stratus clouds (Fig. 7). Despite that, the new criterion is apparently able to detect when embryonic drizzle forms because of strong updrafts in the cloud (Fig. 13); drizzle seeding pixels are identified in the updraft region in the cloud, the V_d distribution is peaking at $-1\,\mathrm{m\,s^{-1}}$ and more than 75% of the pixels have $V_d < 0\,\mathrm{m\,s^{-1}}$. The described signatures visible in the histograms of the different classes from the new criterion cannot be found in the Cloudnet categories. Cloud droplets and drizzle/rain monomodal Z_e distributions peak around $-30\,\mathrm{dB}Z$, while drizzle/rain and cloud droplets category has a bimodal distribution, which peaks as expected at -30 (cloud contribution) and $-10\,\mathrm{dB}Z$ (drizzle contribution). Very broad distributions are obtained by all the categories for V_d and S_w which do not provide additional information.

b. Statistic over a large dataset at JOYCE

We analyze a subset of 378 JOYCE-CF hours of the 500-h dataset presented in Table 2. Every pixels detected by the new criterion is also classified by the Cloudnet target classification algorithm (see Table 3). The CLADS classes are consistent with what one might expect from different stages of drizzle evolution with a progressive shift toward larger reflectivities from $-40\,\mathrm{dB}Z$ for nondrizzle to $-10\,\mathrm{dB}Z$ for drizzle mature. In contrast, the Cloudnet algorithm is based on the usage of a Z_e threshold at $-30\,\mathrm{dB}Z$ for the identification of drizzle in the cloud (see the appendix for more details on the Cloudnet algorithm); the threshold approach results in the shape of the distributions obtained for Z_e in Fig. 14: 75% of cloud droplets only pixels have Z_e smaller than $-31\,\mathrm{dB}Z$, while 75% of drizzle/rain and cloud droplets have

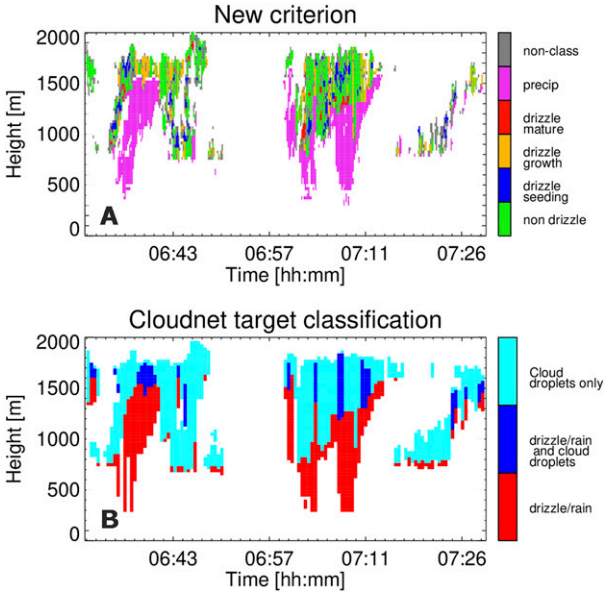

FIG. 12. As in Fig. 6, but for the shallow cumulus cloud over BCO on 11 Dec 2013.

$Z_e > -25$ dBZ; drizzle/rain spans over the whole range of Z_e.

The V_d and S_w distributions for drizzle growth and drizzle mature are consistent with the more advanced stage of drizzle formation, that is, with the presence of larger drizzle drops. The drizzle mature pixels are falling faster than the other classes, with 50% of pixels with $V_d > 0.52\,\mathrm{m\,s^{-1}}$. For the drizzle growth distribution, more than 50% of pixels have $V_d > 0.37\,\mathrm{m\,s^{-1}}$ even if the maximum is at $0\,\mathrm{m\,s^{-1}}$. In terms of Doppler spectrum width, drizzle mature S_w distribution peaks at $0.25\,\mathrm{m\,s^{-1}}$ with 25% of values larger than $0.32\,\mathrm{m\,s^{-1}}$. Also 25% of the values of the drizzle growth distribution are larger than $0.3\,\mathrm{m\,s^{-1}}$. There are two main reasons for the larger Doppler spectrum width values for these two classes: first, Doppler spectra derived when cloud droplets coexist with drizzle are broader due to the presence of two separated peaks in the spectrum. Second, turbulence can foster drizzle formation and drizzle may grow to larger sizes. Hence, larger turbulence in the cloud broadens the spectra, increasing the Doppler spectrum width. Nondrizzle and drizzle seeding classes are the classes corresponding to absence of drizzle droplets and embryonic cloud droplets growth, respectively. The only observed difference between the two classes with respect to the Z_e distributions, with drizzle seeding's Z_e values approximately 5 dBZ larger than nondrizzle. This ''potential precipitation'' is not resolved by the current Cloudnet algorithm. The Cloudnet approach to drizzle detection results in a homogeneous transition from a nondrizzle state (small Z_e and S_w and zero V_d) to a precipitation state (large Z_e and S_w and positive V_d). In Cloudnet, cloud droplets do not fall, while mean V_d for the distribution of drizzle/rain and cloud droplets is $0.38\,\mathrm{m\,s^{-1}}$ and for drizzle/rain is $0.65\,\mathrm{m\,s^{-1}}$. Drizzle/rain and drizzle/rain and cloud droplets are also the categories where larger values of Doppler spectrum width occur, both with 25% of pixels having $S_w > 0.31$, while 75% of cloud droplets only have values $<0.23\,\mathrm{m\,s^{-1}}$.

c. *Indirect evaluation using independent LWP observations at JOYCE*

An independent evaluation of the drizzle detection criterion is done using the LWP measurements of a microwave radiometer. We perform the analysis over the entire dataset of 500 h (see Table 2). For each drizzle class, we determine the percentage of pixels between cloud base and cloud top that belongs to the class for each column. We group the percentages of occurrence of each drizzle class to intervals (0%–20%, 20%–40%, 40%–60%, 60%–80%, and 80%–100%) and for each interval we analyze the distribution of LWP values (Fig. 15). Because the likelihood of drizzle formation increases with LWP, this approach allows an independent evaluation of the classification. When nondrizzle pixels represent more than 50% of the cloudy column, the median LWP is smaller than $50\,\mathrm{g\,m^{-2}}$, which is a typical value occurring for nonprecipitating continental clouds. The drizzle seeding class is expected to catch situations in which drizzle droplets are in an embryonic state and hence no strong increase in LWP is observed; no matter how many drizzle seeding pixels are in the column, the median observed LWP never exceeds $150\,\mathrm{g\,m^{-2}}$. Conversely, columns with more than 20% of drizzle growth pixels have a median LWP around $200\,\mathrm{g\,m^{-2}}$. The identification of the larger drizzle drops by the drizzle mature class is consistent with the observed median LWP values. If more than 20% of the pixels in the column are classified as drizzle mature, LWP grows above $200\,\mathrm{g\,m^{-2}}$, with peaks of 300–$350\,\mathrm{g\,m^{-2}}$ when the percentage of drizzle mature pixels is more than 60%. Finally LWP is around $150\,\mathrm{g\,m^{-2}}$ when just a few unclassified pixels are present in the column. These large LWP values may be due to sporadic pixels that are excluded by the skewness mask in drizzling areas, for example, due to high turbulence. However, when more than 40% of the discarded pixels are in the column, the LWP decreases below $25\,\mathrm{g\,m^{-2}}$. This result shows that the criterion has difficulties in classifying clouds with very small liquid water amounts, which are also geometrically thin. In such cases it is challenging to identify continuous areas of homogeneous skewness values. Finally, when discarded pixels are present for more than 40% of the

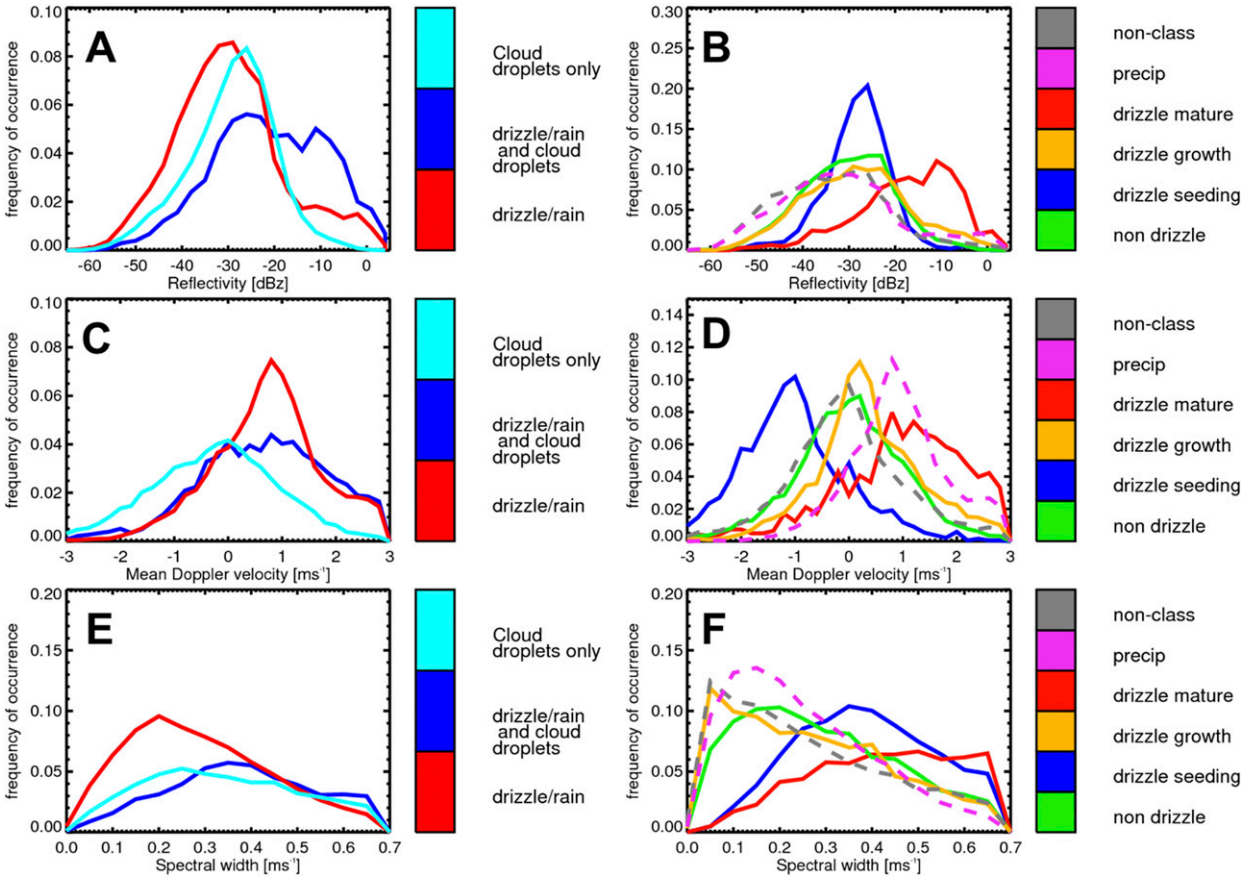

FIG. 13. As in Fig. 7, but for the shallow cumulus cloud over BCO on 11 Dec 2013.

column, LWP is very low, indicating that it is unlikely that they may contain drizzle. This result may indicate that these are nondrizzle pixels. All in all, the statistical comparison with LWP shows that the drizzle classification with CLADS is physically consistent. Table 4 provides a characterization of the drizzle classes in terms of LWP.

5. Conclusions and future work

We introduce a new algorithm (CLADS) to detect drizzle development in liquid clouds using ground-based cloud radars. The algorithm is developed and tested at the JOYCE-CF facility and at the Barbados Cloud Observatory. The inputs needed by the algorithm are skewness, mean Doppler velocity, reflectivity gradients fields, and cloud-base and cloud-top heights. The algorithm is able to identify coherent structures in space and time of positive (drizzle seeding), negative (drizzle mature), and zero (nondrizzle/drizzle growth) skewness using a threshold of ±0.3. The separation between nondrizzle and drizzle growth is based on the reflectivity gradient, which is assumed to be adiabatic for nondrizzling clouds. Precipitation below cloud base is identified by pixels of nonnull mean Doppler velocity. Using case studies and statistical analysis of 500-h cloud observations, we show that the criterion is able to detect regions with potential drizzle formation at an earlier stage than the Cloudnet target classification. Moreover, the new criterion is able to provide a geospatial collocation in time/height of the different drizzle areas in the cloud.

TABLE 2. Statistical properties of the dataset used for analysis of higher moments of Doppler spectra. During the selected hours, single-layer liquid clouds were overpassing the JOYCE-CF site.

Quantity	Value
Total No. of days	45
Total No. of hours	500
Days in summer	19
Days in winter	8
Days in spring	5
Days in autumn	13

TABLE 3. Statistical properties of the ensemble of case studies used for the 1 to 1 comparison with Cloudnet.

	Value	Percentage of the total
Total No. of pixels	13 378 154	
Nondrizzle	3 486 170	26.1%
Drizzle seeding	1 584 212	11.8%
Drizzle growth	2 368 562	17.7%
Drizzle mature	1 268 030	9.5%
Nonclassified	3 214 521	24.0%
Precipitating	1 456 659	10.9%
Cloud droplets only	7 494 496	56%
Drizzle/rain and cloud droplets	3 915 777	29.3%
Drizzle/rain	1 327 174	9.9%
Clear sky	640 707	4.8%

Each stage of drizzle development shows distinct features in terms of reflectivity, mean Doppler velocity, and Doppler spectrum width. CLADS is also able to reveal dynamical mechanisms of drizzle initiation: in the presented case study from Barbados, areas identified as drizzle seeding correspond to the strongest updrafts in the cloud, indicating that the embryonic drizzle formation is initiated by the strong updraft flow.

A detailed analysis of the results also shows that turbulence can dampen the skewness signal; this may result in an increased amount of nonclassified bins. The high resolution of the radar observations is key to exploit the full potential of the skewness observations and minimize the impact of turbulence (Acquistapace et al. 2017). Moreover, we show that the discrimination between nondrizzle and drizzle growth classes based on the slope of the reflectivity profile is an open challenge in some cases, that is, for the maritime clouds or for some continental vertical profiles. This might be also due to the larger integration times used. CLADS has also been validated using independent LWP observations demonstrating its physical consistency. Future work may focus on developing new techniques to properly separate nondrizzle areas from drizzle growth areas. Quantifying turbulence with radar (i.e., Borque et al. 2016; Shupe et al. 2012) and combining this with the presence of drizzle seeding areas above and drizzle

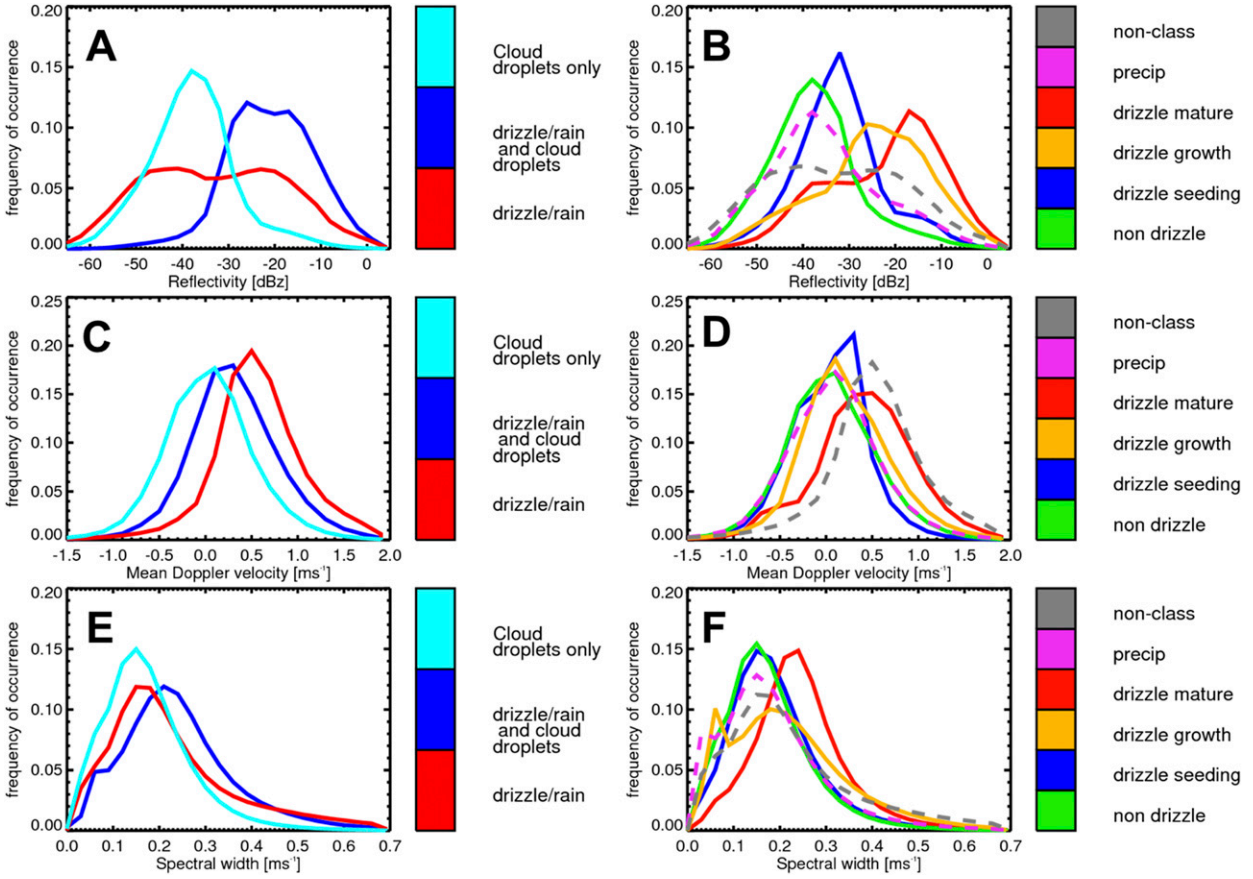

FIG. 14. As in Fig. 7, but for the entire 500-h dataset collected at JOYCE-CF.

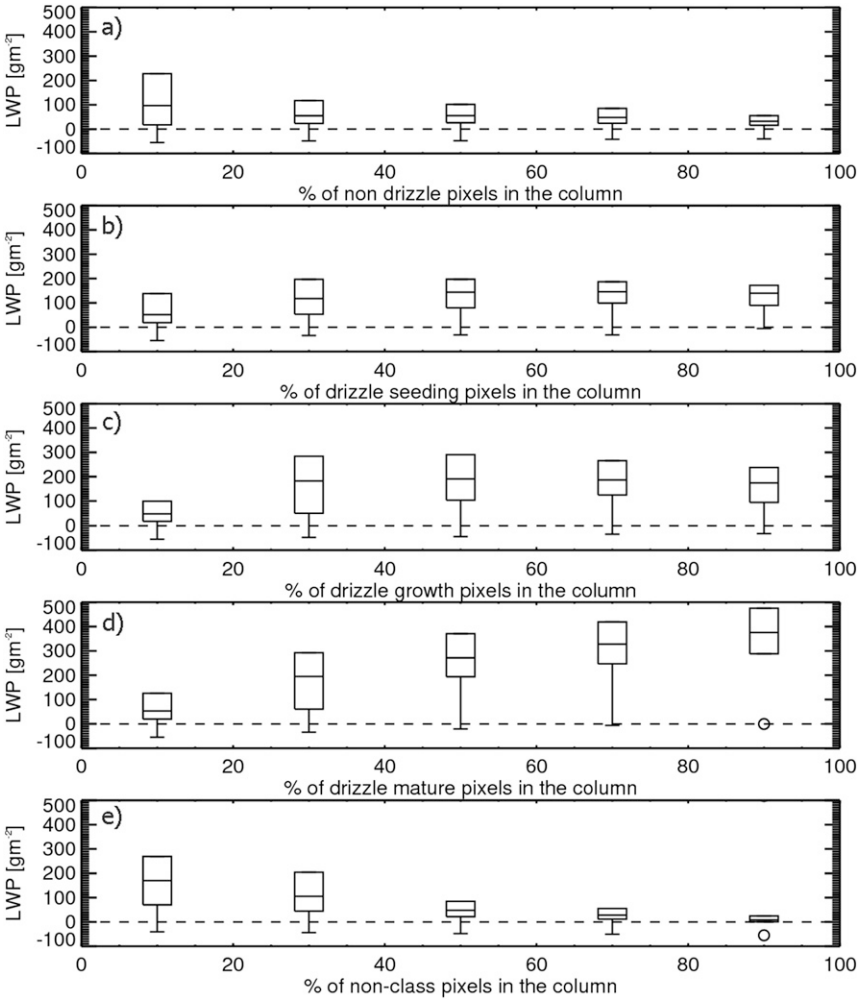

FIG. 15. (a) LWP percentiles for 500-h dataset collected at JOYCE-CF calculated from fixed percentages of nondrizzle pixels between cloud base and cloud top. (b) As in (a), but for drizzle onset pixels, (c) as in (a), but for drizzle growth pixels, (d) as in (a), but for drizzle mature pixels, and (e) as in (a), but for discarded pixels.

mature areas below the drizzle growth region may be of help in this direction. We plan, as a further step, to develop a filtering for pixels that are too turbulent, based on radar-based retrievals of eddy dissipation rates. The presented criterion is currently being implemented as an additional Cloudnet product. This new tool may become valuable for future ground-based validation of upcoming satellite missions, for example, the satellite mission Earth Clouds, Aerosol and Radiation Explorer (EarthCARE) from the European Space Agency (ESA) which is scheduled for launch in 2021. The mission aims at collecting global profiles of cloud, aerosol, and precipitation (Illingworth et al. 2015) which may be validated using ground-based observations and algorithms like CLADS. Moreover, Cloudnet is often used for validating general circulation models (GCMs) (e.g., Ahlgrimm and Forbes 2014) and the improvement in drizzle detection can be beneficial for representing boundary layer clouds and drizzle better in climate models by improving the autoconversion parameterizations. Also, the criterion represents a very powerful potential tool to quantify the drizzle suppression due to the increased aerosol loading.

TABLE 4. Characterization of drizzle classes in terms of LWP.

Class	LWP
Nondrizzle	$<50\,\mathrm{g\,m^{-2}}$
Drizzle onset	$50–150\,\mathrm{g\,m^{-2}}$
Drizzle growth	$100–200\,\mathrm{g\,m^{-2}}$
Drizzle mature	$>200\,\mathrm{g\,m^{-2}}$

Acknowledgments. We thank four anonymous reviewers for their valuable comments and suggestions, which produced an improved version of the manuscript. Observations originate from the DFG-funded Core Facility (JOYCE-CF) under DFG Research Grant LO 901/7-1 and from the Barbados Cloud Observatory operated by Tropical Cloud Observations group of the Max Planck Institute for Meteorology in Hamburg. Data from the Cloudnet project [part of the EU H2020 Project European Research Infrastructure for the observation of Aerosol, Clouds, and Trace gases (ACTRIS)] were exploited for the realization of this work. All data used for this study are available on request from the corresponding author. This study was funded by the German research initiative High Definition Clouds and Precipitation for advancing Climate Prediction [HD(CP)2] II under Grant 01LK1504A through the German Ministry for Education and Research (BMBF). Maximilian Maahn was supported by the U.S. Department of Energy (DOE) Atmospheric Systems Research (ASR) program (DE-SC0013306) and the National Oceanic and Atmospheric Administration (NOAA) Physical Sciences Division (PSD). Finally, we want to acknowledge Dr. Ewan O'Connor from the Finnish Meteorological Institute (FMI) for his contribution to this work and its developments.

APPENDIX

Cloudnet Target Categorization Algorithm for Drizzle Detection

The target Cloudnet categorization is a product of the Cloudnet suite. For the exact description of the algorithm please refer to Hogan and O'Connor (2004). Here, a simplified summary valid only for the liquid cloud case is presented. The target classification classifies each radar range bin (called pixels) in terms of its content of liquid droplets, ice, aerosols, and insects. Since each pixels may contain more than one target simultaneously, the target classification is provided as a bit field. For defining the bits, the radar reflectivity Z_e, the radar mean Doppler velocity V_d, and the lidar backscatter coefficient β' are used. The categories of the target Cloudnet classification dealing with drizzle presence are cloud droplets only, drizzle/rain and cloud droplets, and drizzle/rain and each one of them corresponds to a given combination of bits. The bits defining these categories are as follows:

1) Bit 0 or droplet bit (only cloud droplets present): Cloud base is identified by the lidar backscattering β', while cloud top is identified by radar reflectivity or lidar backscatter when it is not extinguished. Then droplet bit is set to 1 for all pixels between cloud base and cloud top.
2) Bit 1 or falling bit (precipitation present): To assign the falling bit the Z_e profile is used. The ΔZ_e quantity is defined as the difference between the Z_e value at a height 20% below cloud top and the Z_e value at a height 20% above cloud base; $\Delta Z_e > 0$ corresponds to a nondrizzling profile, while $\Delta Z_e < 0$ implies drizzle presence. The falling bit is set to 1 for all pixels between cloud base and cloud top where $Z_e > -30$ dBZ and whose column has $\Delta Z_e < 0$.
3) Bit 2 or phase bit (cold/melting bit): It assigns the phase of a bit by checking the wet-bulb temperature and the Doppler velocity V_d. Liquid phase has wet-bulb temperature >0°C. Sharp increase in V_d is observed at the melting layer thus combining these two features ice phase is distinguished from liquid phase.

The combinations of bits resulting in the aforementioned categories for the Cloudnet target categorization are as follows:

- Cloud droplets only: bit 0 = 1, bit 1 = 0, bit 2 = 0
- Drizzle/rain and cloud droplets: bit 0 = 1, bit 1 =1, bit 2 = 0
- Drizzle/rain: bit 0 = 0, bit 1 = 1, bit 2 = 0

REFERENCES

Acquistapace, C., 2017: Investigation of drizzle onset in liquid clouds using ground based active and passive remote sensing instruments. Ph.D. thesis, University of Cologne, 199 pp., http://kups.ub.uni-koeln.de/7932/.

——, S. Kneifel, U. Löhnert, P. Kollias, M. Maahn, and M. Bauer-Pfundstein, 2017: Optimizing observations of drizzle onset with millimeter-wavelength radars. *Atmos. Meas. Tech.*, **10**, 1783–1802, https://doi.org/10.5194/amt-10-1783-2017.

Ahlgrimm, M., and R. Forbes, 2014: Improving the representation of low clouds and drizzle in the ECMWF model based on ARM observations from the Azores. *Mon. Wea. Rev.*, **142**, 668–685, https://doi.org/10.1175/MWR-D-13-00153.1.

Bony, S., and Coauthors, 2006: How well do we understand and evaluate climate change feedback processes? *J. Climate*, **19**, 3445–3482, https://doi.org/10.1175/JCLI3819.1.

Borque, P., E. Luke, and P. Kollias, 2016: On the unified estimation of turbulence eddy dissipation rate using Doppler cloud radars and lidars. *J. Geophys. Res. Atmos.*, **121**, 5972–5989, https://doi.org/10.1002/2015JD024543.

Doviak, R., and D. Zrnić, 1993: *Doppler Radar and Weather Observations*. 2nd ed. Academic Press, 562 pp.

Franklin, C. N., 2008: A warm rain microphysics parameterization that includes the effect of turbulence. *J. Atmos. Sci.*, **65**, 1795–1816, https://doi.org/10.1175/2007JAS2556.1.

Frisch, A. S., C. Fairall, and J. Snider, 1995a: Measurement of stratus cloud and drizzle parameters in ASTEX with a K-band Doppler radar and a microwave radiometer. *J. Atmos. Sci.*, **52**,

2788–2799, https://doi.org/10.1175/1520-0469(1995)052<2788:MOSCAD>2.0.CO;2.

——, D. H. Lenschow, C. W. Fairall, W. H. Schubert, and J. S. Gibson, 1995b: Doppler radar measurements of turbulence in marine stratiform cloud during ASTEX. *J. Atmos. Sci.*, **52**, 2800–2808, https://doi.org/10.1175/1520-0469(1995)052<2800:DRMOTI>2.0.CO;2.

Hogan, R. J., and E. J. O'Connor, 2004: Facilitating cloud radar and lidar algorithms: The Cloudnet instrument synergy/target categorization product. University of Reading Rep., 14 pp., http://www.met.rdg.ac.uk/~swrhgnrj/publications/categorization.pdf.

——, M. P. Mittermaier, and A. J. Illingworth, 2006: The retrieval of ice water content from radar reflectivity factor and temperature and its use in evaluating a mesoscale model. *J. Appl. Meteor. Climatol.*, **45**, 301–317, https://doi.org/10.1175/JAM2340.1.

Hsieh, W. C., H. Jonsson, L.-P. Wang, G. Buzorius, R. C. Flagan, J. H. Seinfeld, and A. Nenes, 2009: On the representation of droplet coalescence and autoconversion: Evaluation using ambient cloud droplet size distributions. *J. Geophys. Res.*, **114**, D07201, https://doi.org/10.1029/2008JD010502.

Illingworth, A. J., and Coauthors, 2007: Cloudnet: Continuous evaluation of cloud profiles in seven operational models using ground-based observations. *Bull. Amer. Meteor. Soc.*, **88**, 883–898, https://doi.org/10.1175/BAMS-88-6-883.

——, and Coauthors, 2015: The EarthCARE Satellite: The next step forward in global measurements of clouds, aerosols, precipitation, and radiation. *Bull. Amer. Meteor. Soc.*, **96**, 1311–1332, https://doi.org/10.1175/BAMS-D-12-00227.1.

Kessler, E., 1969: *On the Distribution and Continuity of Water Substance in Atmospheric Circulation*. *Meteor. Monogr.*, Vol. 10. Amer. Meteor. Soc., 84 pp., https://doi.org/10.1007/978-1-935704-36-2_1.

Khairoutdinov, M., and Y. Kogan, 2000: A new cloud physics parameterization in a large-eddy simulation model of marine stratocumulus. *Mon. Wea. Rev.*, **128**, 229–243, https://doi.org/10.1175/1520-0493(2000)128<0229:ANCPPI>2.0.CO;2.

Kogan, Z. N., D. B. Mechem, and Y. L. Kogan, 2005: Assessment of variability in continental low stratiform clouds based on observations of radar reflectivity. *J. Geophys. Res.*, **110**, D18205, https://doi.org/10.1029/2005JD006158.

Kollias, P., J. Rémillard, E. Luke, and W. Szyrmer, 2011a: Cloud radar Doppler spectra in drizzling stratiform clouds: 1. Forward modeling and remote sensing applications. *J. Geophys. Res.*, **116**, D13201, https://doi.org/10.1029/2010JD015237.

——, W. Szyrmer, J. Rémillard, and E. Luke, 2011b: Cloud radar Doppler spectra in drizzling stratiform clouds: 2. Observations and microphysical modeling of drizzle evolution. *J. Geophys. Res.*, **116**, D13203, https://doi.org/10.1029/2010JD015238.

L'Ecuyer, T. S., W. Berg, J. Haynes, M. Lebsock, and T. Takemura, 2009: Global observations of aerosol impacts on precipitation occurrence in warm maritime clouds. *J. Geophys. Res.*, **114**, D09211, https://doi.org/10.1029/2008JD011273.

Liu, Y., and P. H. Daum, 2004: Parameterization of the autoconversion process. Part I: Analytical formulation of the Kessler-type parameterizations. *J. Atmos. Sci.*, **61**, 1539–1548, https://doi.org/10.1175/1520-0469(2004)061<1539:POTAPI>2.0.CO;2.

——, B. Geerts, M. Miller, P. Daum, and R. McGraw, 2008: Threshold radar reflectivity for drizzling clouds. *Geophys. Res. Lett.*, **35**, L03807, https://doi.org/10.1029/2007GL031201.

Löhnert, U., and S. Crewell, 2003: Accuracy of cloud liquid water path from ground-based microwave radiometry 1. Dependency on cloud model statistics. *Radio Sci.*, **38**, 8041, https://doi.org/10.1029/2002RS002654.

——, and Coauthors, 2015: JOYCE: Jülich Observatory for Cloud Evolution. *Bull. Amer. Meteor. Soc.*, **96**, 1157–1174, https://doi.org/10.1175/BAMS-D-14-00105.1.

Luke, E. P., and P. Kollias, 2013: Separating cloud and drizzle radar moments during precipitation onset using Doppler spectra. *J. Atmos. Oceanic Technol.*, **30**, 1656–1671, https://doi.org/10.1175/JTECH-D-11-00195.1.

Mace, G. G., and K. Sassen, 2000: A constrained algorithm for retrieval of stratocumulus cloud properties using solar radiation, microwave radiometer, and millimeter cloud radar data. *J. Geophys. Res.*, **105**, 29 099–29 108, https://doi.org/10.1029/2000JD900403.

Miles, N. L., J. Verlinde, and E. E. Clothiaux, 2000: Cloud droplet size distributions in low-level stratiform clouds. *J. Atmos. Sci.*, **57**, 295–311, https://doi.org/10.1175/1520-0469(2000)057<0295:CDSDIL>2.0.CO;2.

Münkel, C., N. Eresmaa, J. Räsänen, and A. Karppinen, 2007: Retrieval of mixing height and dust concentration with lidar ceilometer. *Bound.-Layer Meteor.*, **124**, 117–128, https://doi.org/10.1007/s10546-006-9103-3.

O'Connor, E. J., R. J. Hogan, and A. J. Illingworth, 2005: Retrieving stratocumulus drizzle parameters using Doppler radar and lidar. *J. Appl. Meteor.*, **44**, 14–27, https://doi.org/10.1175/JAM-2181.1.

Randall, D., J. Coakley Jr., D. Lenschow, C. Fairall, and R. Kropfli, 1984: Outlook for research on subtropical marine stratification clouds. *Bull. Amer. Meteor. Soc.*, **65**, 1290–1301, https://doi.org/10.1175/1520-0477(1984)065<1290:OFROSM>2.0.CO;2.

Rapp, A. D., M. Lebsock, and T. L'Ecuyer, 2013: Low cloud precipitation climatology in the southeastern Pacific marine stratocumulus region using CloudSat. *Environ. Res. Lett.*, **8**, 014027, https://doi.org/10.1088/1748-9326/8/1/014027.

Rose, T., S. Crewell, U. Löhnert, and C. Simmer, 2005: A network suitable microwave radiometer for operational monitoring of the cloudy atmosphere. *Atmos. Res.*, **75**, 183–200, https://doi.org/10.1016/j.atmosres.2004.12.005.

Seifert, A., and K. Beheng, 2006: A two-moment cloud microphysics parameterization for mixed-phase clouds. Part 1: Model description. *Meteor. Atmos. Phys.*, **92**, 45–66, https://doi.org/10.1007/s00703-005-0112-4.

Shupe, M. D., P. Kollias, S. Y. Matrosov, and T. L. Schneider, 2004: Deriving mixed-phase cloud properties from Doppler radar spectra. *J. Atmos. Oceanic Technol.*, **21**, 660–670, https://doi.org/10.1175/1520-0426(2004)021<0660:DMCPFD>2.0.CO;2.

——, I. Brooks, and G. Canut, 2012: Evaluation of turbulent dissipation rate retrievals from Doppler cloud radar. *Atmos. Meas. Tech.*, **5**, 1375–1385, https://doi.org/10.5194/amt-5-1375-2012.

Siebert, H., and Coauthors, 2013: The fine-scale structure of the trade wind cumuli over Barbados—An introduction to the CARRIBA project. *Atmos. Chem. Phys.*, **13**, 10 061–10 077, https://doi.org/10.5194/acp-13-10061-2013.

Stephens, G. L., and J. M. Haynes, 2007: Near global observations of the warm rain coalescence process. *Geophys. Res. Lett.*, **34**, L20805, https://doi.org/10.1029/2007GL030259.

Stevens, B., and Coauthors, 2016: The Barbados Cloud Observatory: Anchoring investigations of clouds and circulation on the edge of the ITCZ. *Bull. Amer. Meteor. Soc.*, **97**, 787–801, https://doi.org/10.1175/BAMS-D-14-00247.1.

Suzuki, K., T. Y. Nakajima, and G. L. Stephens, 2010: Particle growth and drop collection efficiency of warm clouds as inferred from joint *CloudSat* and MODIS observations.

J. Atmos. Sci., **67**, 3019–3032, https://doi.org/10.1175/2010JAS3463.1.

Tripoli, G. J., and W. R. Cotton, 1980: A numerical investigation of several factors contributing to the observed variable intensity of deep convection over south Florida. *J. Appl. Meteor.*, **19**, 1037–1063, https://doi.org/10.1175/1520-0450(1980)019<1037:ANIOSF>2.0.CO;2.

Vogelmann, A. M., and Coauthors, 2012: RACORO extended-term aircraft observations of boundary layer clouds. *Bull. Amer. Meteor. Soc.*, **93**, 861–878, https://doi.org/10.1175/BAMS-D-11-00189.1.

Westbrook, C. D., R. J. Hogan, E. J. O'Connor, and A. J. Illingworth, 2010: Estimating drizzle drop size and precipitation rate using two-colour lidar measurements. *Atmos. Meas. Tech.*, **3**, 671–681, https://doi.org/10.5194/amt-3-671-2010.

Wood, R., 2005: Drizzle in stratiform boundary layer clouds. Part II: Microphysical aspects. *J. Atmos. Sci.*, **62**, 3034–3050, https://doi.org/10.1175/JAS3530.1.

Yang, F., E. P. Luke, P. Kollias, A. B. Kostinski, and A. M. Vogelmann, 2018: Scaling of drizzle virga depth with cloud thickness for marine stratocumulus clouds. *Geophys. Res. Lett.*, **45**, 3746–3753, https://doi.org/10.1029/2018GL077145.